ANALYSIS OF THE BANDWIDTH PERFORMANCE OF SIS MIXERS WITH DISTRIBUTED JUNCTION ARRAYS

Sheng-Cai Shi, Takashi Noguchi, and Junji Inatani

Nobeyama Radio Observatory
National Astronomical Observatory of Japan
Nobeyama, Minamisaku, Nagano, 384-13 Japan
E-mail: shencai@nro.nao.ac.jp; noguchi@; intani@

ABSTRACT: In this paper, the bandwidth performance of the distributed junction array, i.e., a number of junctions connected in parallel with a tuning inductance separating every two junctions, is theoretically investigated. The small-signal equivalent circuit model of the distributed junction array is constructed in a general form of multi-sideband frequency ports in order to employ the quantum theory of mixing. Detailed simulation results are presented.

I. INTRODUCTION

Broadband SIS-junction devices are of benefit in developing tuneless or fixed-tuned mixers that are highly desirable at submillimeter wavelengths and for complex systems such as multibeam receivers and interferometer arrays. Typically, submillimeter SIS mixers use junctions of a relatively large $\omega R_n C_j$ product (say 4), as far as the junction's critical current density (J_c), which is limited to around 10 kA/cm^2 for Nb junctions, is concerned. The bandwidth of such SIS mixers is governed mainly by the $\omega R_n C_j$ product, i.e., approximately the Q-factor of the resonance circuit tuning out the junction capacitance. Recently, Tong et al. [1] proposed a junction device made of a nonlinear thin-film transmission line, which has demonstrated encouraging performance (less J_c-independence, large bandwidth, and low noise). Such a type of junction, however, has a very small line-width (~0.1 μm), requiring the electron-beam lithograph for the junction fabrication.

Here we propose another type of junction device, i.e., the distributed junction array made up of a number of junctions connected in parallel with a tuning inductance separating every two junctions. In practice, the distributed junction array is the extension of conventional twin-junction devices [2-3].

II. THEORETICAL MODEL OF DISTRIBUTED JUNCTION ARRAYS

The distributed junction array, as illustrated in Fig. 1, appears like a lossy transmission line as a single junction can be approximately regarded as the parallel combination of a resistance and capacitance. It has only a single port, feeding both the RF and LO signals. All the junctions in such an array are dc-biased at the same voltage. While an LO signal is applied,

however, the SIS junctions must be impressed by different LO voltages (in both amplitude and phase, appearing frequency dependent) due to the phase shift by the tuning inductance, thereby having different small-signal characteristics. Nevertheless, it would be straightforward to simulate the mixing behavior of distributed junction arrays using the quantum theory of mixing, while their equivalent conversion admittance and noise correlation matrices are constructed. A method similar to that in [2-3] is adopted here.

II.a LO-voltage distribution

To understand the distribution of the LO voltage in a distributed junction array, strictly speaking, it is necessary to carry out a large-signal analysis. Here we employ a simple method, i.e., assuming a sinusoidal LO voltage applied to each junction, as it has been very effective in simulating SIS mixers, especially for those using SIS junctions of a considerably large capacitance (a typical case for submillimeter SIS mixers).

Fig. 2 demonstrates an equivalent circuit for the k-th SIS junction of an N-junction array, including its preceding tuning inductance that is described by a chain matrix $[C]^p$ at the LO frequency ω_p. The LO voltage and current at port $(k\text{-}1)$ (V_p^{k-1}, I_p^{k-1}), i.e., the LO voltage applied to and the LO current flowed out of the $(k\text{-}1)$-th junction, can be written

$$V_p^{k-1} = C_{11,p}V_p^k + C_{12,p}\left[I_p^k + I_{j,p}^k + j\omega_p C_j V_p^k\right] \tag{1}$$

$$I_p^{k-1} = C_{21,p}V_p^k + C_{22,p}\left[I_p^k + I_{j,p}^k + j\omega_p C_j V_p^k\right] \tag{2}$$

where V_p^k and I_p^k denotes the LO voltage and current at port k, respectively, $I_{j,p}^k$ is the LO current induced in the k-th junction (only its intrinsic branch, given by Eq. (4.41) in [4]), C_j is the single-junction's geometric capacitance, and $C_{11,p}$, $C_{12,p}$, $C_{21,p}$, and $C_{22,p}$ are the elements of the chain matrix $[C]^p$. Notice that I_p^k is equal to zero while k=N (i.e., at the last junction). Apparently the LO voltage developed to each junction can be calculated using Eqs. (1-2), once the LO voltage across the last junction, V_p^N, is determined (actually optimized for the SIS mixer performance).

II.b Equivalent conversion admittance matrix

Fig. 3a shows the equivalent circuit of the k-th junction at the m'-th sideband, including its shot-noise current source and an equivalent one representing the shot noise due to all the following junctions. It is assumed that only the small-signal voltage at the m'-th sideband (i.e., $\omega_{m'} = m'\omega_p + \omega_0$, here ω_0 is the IF frequency), $V_{m'}$, is developed to this junction, according to the definition of the conversion admittance matrix

$$Y_{mm'} = \left.\frac{I_m}{V_{m'}}\right|_{V_j=0,\, j\neq m'}, \quad m, m' = \cdots, -2, -1, 0, 1, 2, \cdots \tag{3}$$

where I_m is the small-signal current induced at the m-th sideband (i.e., $\omega_m = m\omega_p + \omega_0$). Let us first omit those noise current sources. The small-signal voltage at port (k-*1*) at the m'-th sideband is therefore given by

$$V_{m'}^{k-1} = C_{11,m'}V_{m'}^{k} + C_{12,m'}\left[I_{m'}^{k} + I_{j,m'}^{k} + j\omega_{m'}C_j V_{m'}^{k}\right] \tag{4}$$

and the small-signal current at port (k-*1*) induced at the m-th sideband by

$$I_{m}^{k-1} = C_{21,m}V_{m'}^{k}\delta_{mm'} + C_{22,m}\left[I_{m}^{k} + I_{j,m}^{k} + j\omega_{m}C_j V_{m'}^{k}\delta_{mm'}\right] \tag{5}$$

Replacing the junction (intrinsic branch) currents $I_{j,m'}^{k}$ and $I_{j,m}^{k}$ with $Y_{m'm'}^{k}V_{m'}^{k}$ and $Y_{mm'}^{k}V_{m'}^{k}$ respectively, and small-signal currents $I_{m'}^{k}$ and I_{m}^{k} with $Y_{m'm',e}^{k}V_{m'}^{k}$ and $Y_{mm',e}^{k}V_{m'}^{k}$, into (4) and (5) and using (3), give the elements of the equivalent conversion admittance matrix at port (k-*1*), $[Y_e^{k-1}]$

$$Y_{mm',e}^{k-1} = \frac{C_{21,m}\delta_{mm'} + C_{22,m}\left[Y_{mm',e}^{k} + Y_{mm'}^{k} + j\omega_m C_j\delta_{mm'}\right]}{C_{11,m'} + C_{12,m'}\left[Y_{m'm',e}^{k} + Y_{m'm'}^{k} + j\omega_{m'}C_j\right]} \tag{6}$$

where $[Y^k]$ and $[Y_e^k]$ are designated as the k-th junction's conversion admittance matrix (defined by QTM [4] for the corresponding LO voltage, including the LO-voltage phase effect [2-3]) and the equivalent conversion admittance matrix at port k, respectively. Notice that $Y_{mm',e}^{N} = 0$ and $Y_{mm',e}^{0}$ represents the elements of the array's equivalent conversion admittance matrix.

II.c Equivalent noise correlation matrix

In terms of the theory of noisy fourpoles [5], the two shot-noise current sources in Fig. 3a can be described by a noise-voltage source $E_{m'}^{k-1}$ and a noise-current source $I_{m'}^{k-1}$ in parallel with the input admittance seen before the chain matrix (refer to Fig. 3b). The magnitudes of the two equivalent noise sources are expressed as

$$E_{m'}^{k-1} = C_{12,m'}\left(I_{s,m'}^{k} + I_{se,m'}^{k}\right) \tag{7}$$

$$I_{m'}^{k-1} = C_{22,m'}\left(I_{s,m'}^{k} + I_{se,m'}^{k}\right) \tag{8}$$

The total short-circuit noise current at port (k-*1*) at the m'-th sideband is therefore written

$$\begin{aligned} I_{se,m'}^{k-1} &= E_{m}^{k-1}Y_{in,m'}^{k-1} - I_{m'}^{k-1} \\ &= \left(C_{12,m'}Y_{m'm',e}^{k-1} - C_{22,m'}\right)\left(I_{s,m'}^{k} + I_{se,m'}^{k}\right) \end{aligned} \tag{9}$$

The correlation matrix of this equivalent noise-current source has elements of this form

$$H_{mm',e}^{k-1} = C_{e,m}C_{e,m'}^{*}\left[H_{mm'}^{k} + H_{mm',e}^{k}\right] \tag{10}$$

where $H^k_{mm'}$ and $H^k_{mm',e}$ are the elements of the k-th junction's shot-noise correlation matrix (defined by QTM [4] for the corresponding LO voltages, including the LO-voltage phase effect [2-3]) and of the equivalent shot-noise correlation matrix at port k, respectively, and $C_{e,m}$ is a transfer factor defined as

$$C_{e,m} = C_{12,m} Y^k_{mm,e} - C_{22,m} \tag{11}$$

It should be pointed out that $H^N_{mm',e} = 0$, and that $H^0_{mm',e}$ and the thermal-noise component at port *0* combine the total noise correlation matrix for the distributed junction array.

III. Simulation Results and Analyses

Using the quantum theory of mixing, together with the equivalent circuit model established above, we have simulated the mixing behavior of the distributed junction array in the frequency range of 100~1000 GHz for three examples of two (a particular case, i.e., twin-junction device), eight, and sixteen junctions, respectively. All the junctions were assumed to have the same critical current density as 3 kA/cm^2 (relatively low for Nb junctions) that corresponds to a $\omega R_n C_j$ product of about eleven at 500 GHz. Therefore, a sharp junction I-V curve of a quality factor of around 35 mV was employed in the simulation. The tuning inductance (L) was studied for three different values, having $\omega L/R_n$ @ 500 GHz equal to .117, .192, and .258 (around its resonance value at 500 GHz) for the twin-junction array but equal to .042, .067, and .092 for the eight- and 16-junction arrays. Assumed a pure resistance and to be identical at all the frequencies, the RF and IF terminations for the three examples had normalized (to the junction array's equivalent normal-state resistance, i.e., R_n/N, here N is the junction number) values of one and ten, respectively. Note that quite a large IF termination was used in conjunction with small values of the junction array's equivalent normal-state resistance (typically of order of several ohms) and the intention of neglecting an IF impedance transformer.

Figs. 4-6 demonstrate the simulated mixer noise temperature and conversion gain for the three examples, respectively. Note that at each frequency the dc-bias and the LO (at the last junction) voltages were optimized for the receiver noise temperature by assuming an IF noise temperature of 10 K. Obviously, with the increase of the junction number, the overall bandwidth performance of the distributed junction array is improved immensely and becoming less insensitive to the tuning inductance. In comparison to the mixer conversion gain, however, the mixer noise temperature degrades rapidly at certain frequencies that may differ according to the junction number, the $\omega R_n C_j$ product, and the tuning inductance. It has been found that these frequencies actually correspond to the minima of the optimized LO voltage seen before the junction array, just as exhibited in Fig. 6b. Increasing the tuning inductance is helpful to the reduction of this fluctuation, but for arrays of a large number of junctions too large an inductance would deteriorate the mixer performance considerably at high frequencies.

Regarding the local bandwidth (i.e., one between two singular frequencies), which is supposed to be of frequency independence according to a constant J_c, it simply decreases with the increase either of frequency or of the junction number. For arrays of the same junction number the smaller the tuning inductance is, the larger local bandwidths become.

Another 16-junction array of the critical current density equal to 6 kA/cm^2, which doubles the one examined before, has also been investigated. The simulation results are displayed in Fig. 7. Apparently the frequency response of the mixer noise temperature is improved in comparison to that in Fig. 6a, while that of the mixer conversion gain is very similar.

It has been concluded that the distributed junction array's bandwidth can be enlarged by increasing either the junction number or the critical current density. The latter, however, is clearly of no benefit in fabricating SIS junctions. And for both cases, the array's input impedance would be reduced so as to make it difficult to match the RF termination. Keeping these in mind, we suggest that the junction number N and critical current density J_c are chosen according to a fixed NJ_c product (say 35 kA/cm^2). Regarding the optimum tuning inductance, it is not so critical for arrays of a large number of junctions and may be determined in terms of the relation, $\omega L/R_n$=0.07 (at 500 GHz).

IV. SUMMARY

The mixing behavior of the distributed junction array has been theoretically investigated. Its bandwidth performance can be improved considerably using a large number of junctions (e.g., >10), and appears insensitive to the tuning inductance in comparison to the case of a single junction. One example, assuming sixteen Nb junctions of the critical current density as low as 3 kA/cm^2, has demonstrated a mixer conversion gain (SSB) of −3.5~−7.5 dB and a mixer noise temperature (SSB) varying from 15 to 150 K over the frequency range of 100~1000 GHz. Hence distributed junction arrays, even composed of very low-J_c junctions, should be of good use for submillimeter-wave SIS mixers.

ACKNOWLEDGMENT

Authors thank Jonas Zmuidzinas for valuable discussions.

REFERENCE

[1] C.E. Tong, R. Blundell, B. Bumble, J.A. Stern, and H.G. LeDuc, "Quantum limited heterodyne detection in superconducting non-linear transmission lines at sub-millimeter wavelengths," *Appl. Phys. Lett.*, vol. 67, pp. 1304-1306, Aug. 1995.

[2] J. Zmuidzinas, H.G. LeDuc, J.A. Stern, and S.R. Cypher, "Two-junction tuning circuits for submillimeter SIS mixers," *IEEE Trans. Microwave Theory Tech.*, vol. 42, no. 4, pp. 698-706, 1994.

[3] T. Noguchi, S.C. Shi, and J. Inatani, "Parallel connected twin junctions for millimeter and submillimeter wave SIS mixers: analysis and experimental verification," *IEICE Trans. Electronics*, vol. E78-c, no. 5, pp. 481-489, May 1995.

[4] J. R. Tucker and M.J. Feldman, "Quantum detection at millimeter wavelengths," *Rec. Mod. Phys.*, vol. 57, no. 4, pp. 1055-1113, Oct. 1985.

[5] H. Rothe and W. Dahlke, "Theory of noisy fourpoles," *Proc. IRE*, vol. 44, pp. 811-818, June 1956.

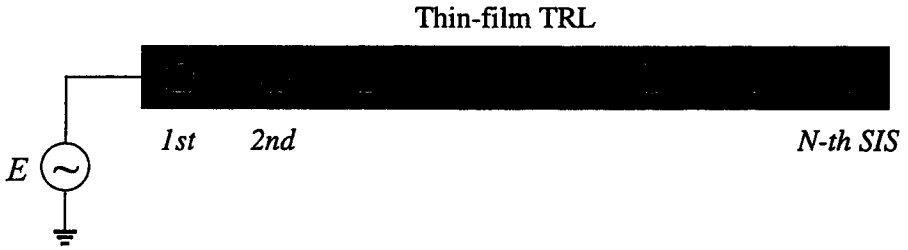

Fig. 1 Schematic of the distributed junction array composed of N junctions. Every two junctions are seperated by a tuning inductance.

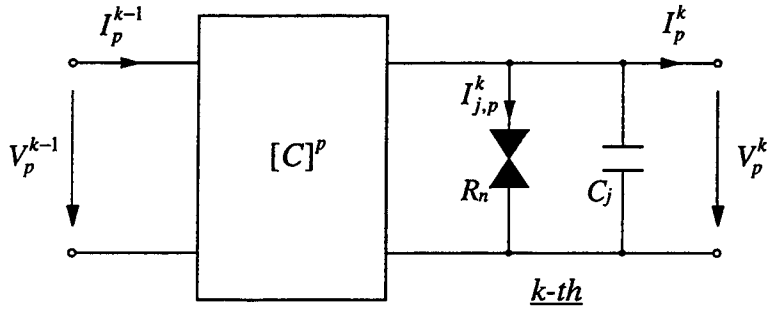

Fig. 2 LO equivalent circuit for the k-th junction and its preceding tuning inductance (described by a chain matrix [C]).

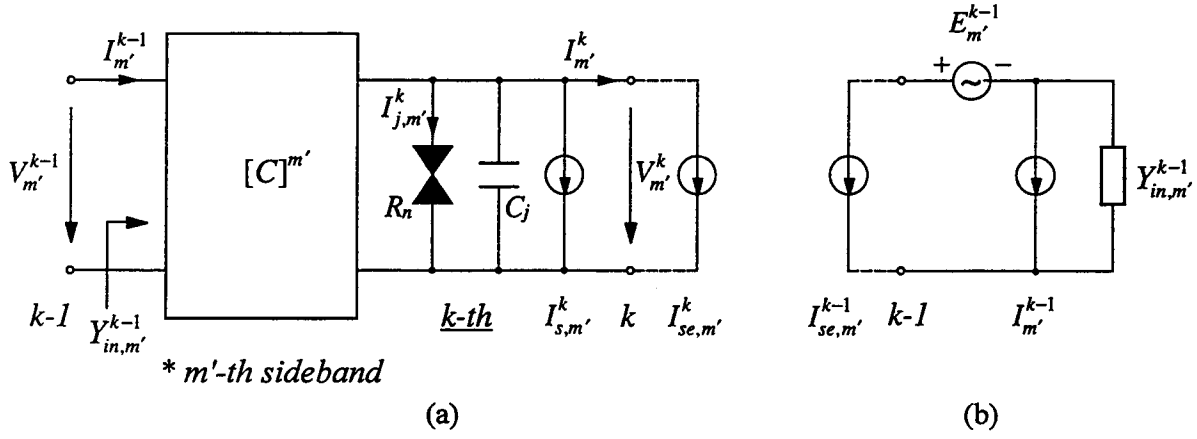

Fig. 3 (a) Small-signal equivalent circuit for the k-th junction and its preceding tuning inductance at the m'-th sideband. (b) Noise equivalent circuit at port (k-1), representing all the shot noise sources due to the k-th and following junctions.

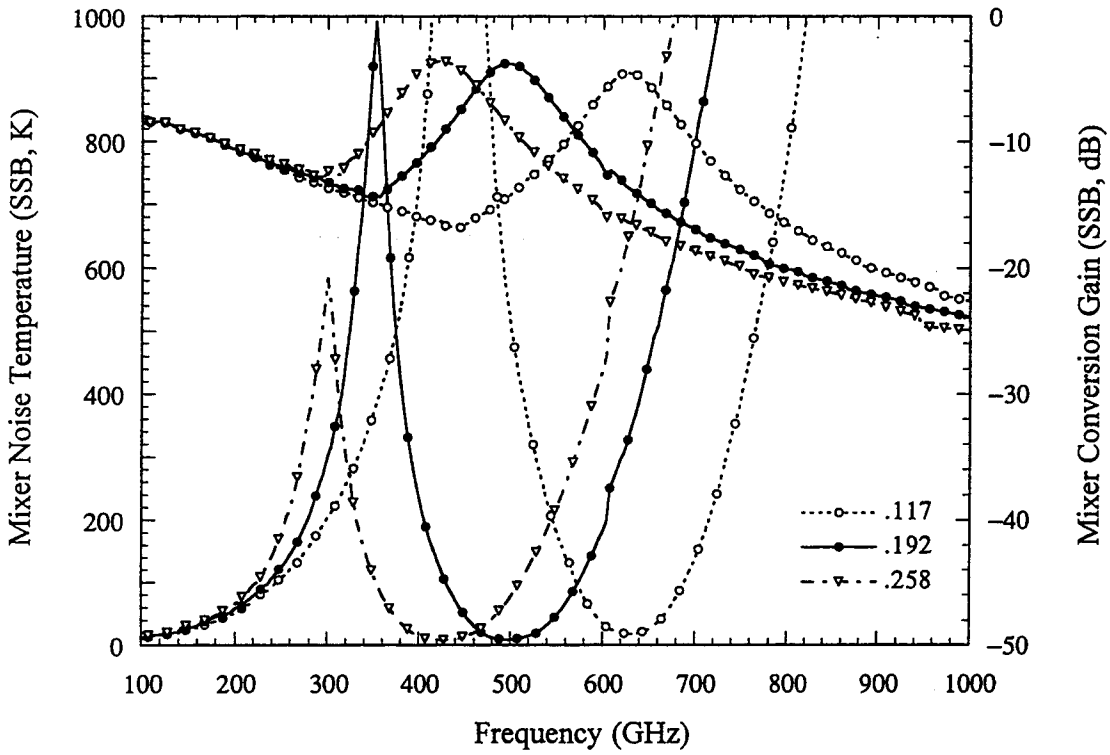

Fig. 4 Simulated mixer noise temperature and conversion gain for a twin-junction (J_c=3kA/cm2) array, as a function of frequency. Results are shown for three inductances (wL/R_n at 500 GHz).

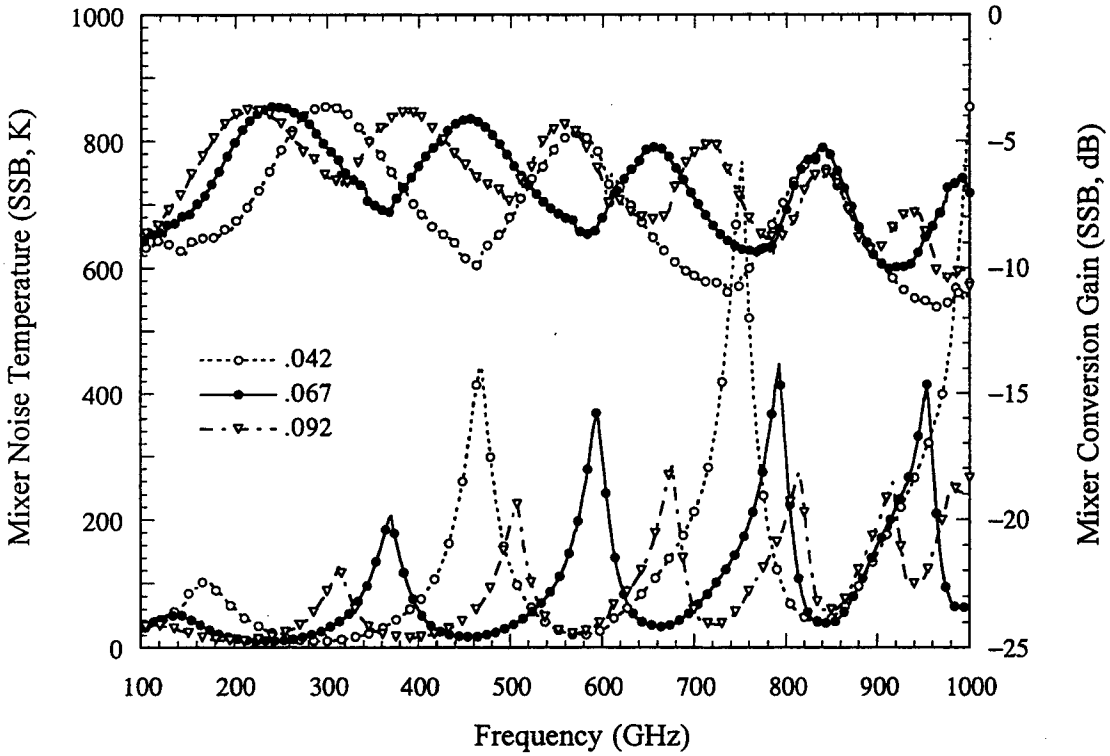

Fig. 5 Simulated mixer noise temperature and conversion gain for a 8-junction (J_c=3kA/cm2) array, as a function of frequency. Results are shown for three inductances (wL/R_n at 500 GHz).

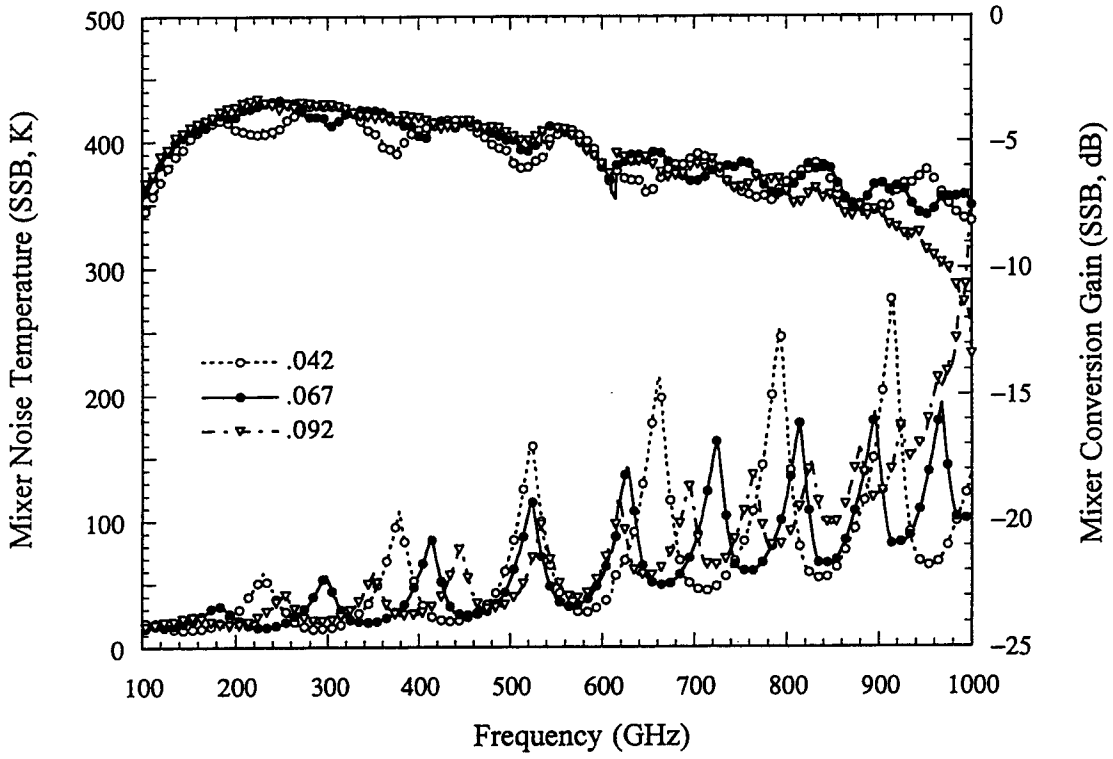

Fig. 6a Simulated mixer noise temperature and conversion gain for a 16-junction (J_c=3kA/cm2) array, as a function of frequency. Results are shown for three inductances (wL/R_n at 500 GHz).

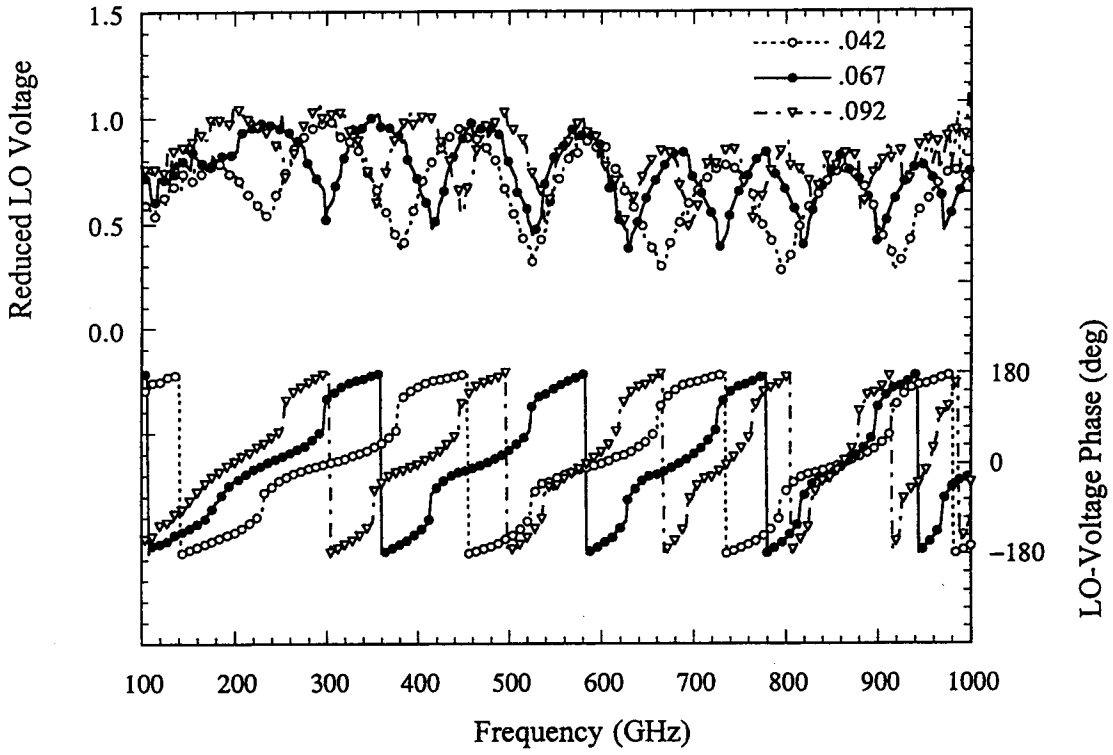

Fig. 6b Optimized LO voltage (magnitude and phase) for a 16-junction (J_c=3kA/cm2) array, as a function of frequency. Results are shown for three inductances (wL/R_n at 500 GHz).

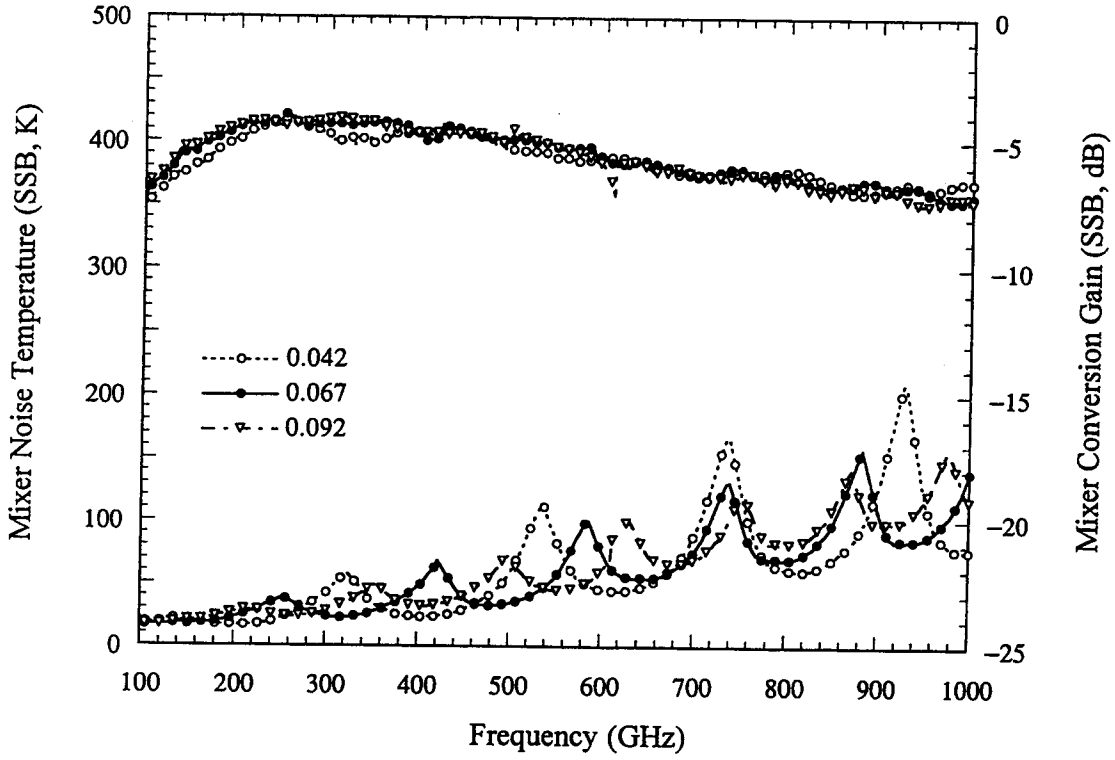

Fig. 7a Simulated mixer noise temperature and conversion gain for a 16-junction (J_c=6kA/cm2) array, as a function of frequency. Results are shown for three inductances (wL/R_n at 500 GHz).

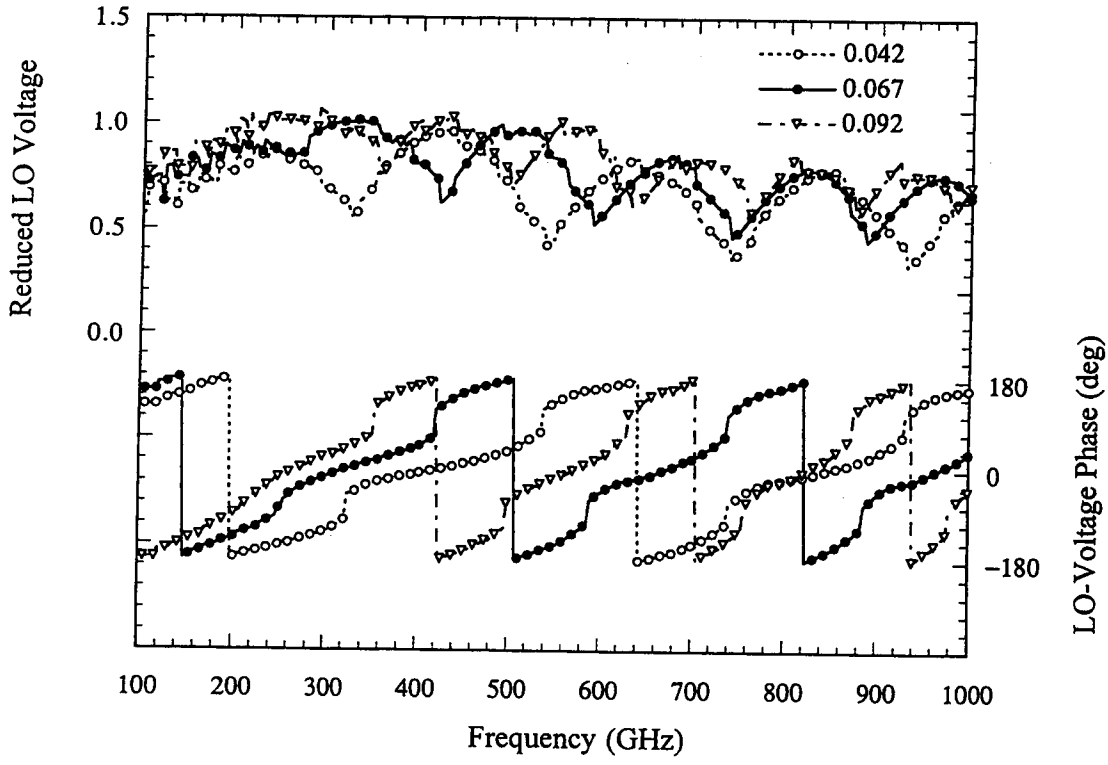

Fig. 7b Optimized LO voltage (magnitude and phase) for a 16-junction (J_c=6kA/cm2) array, as a function of frequency. Results are shown for three inductances (wL/R_n at 500 GHz).